Published in final edited form as:
Inflamm Res. 2015 February ; 64(2): 107–118. doi:10.1007/s00011-014-0789-2.

Esophageal Cancer Related Gene-4 (ECRG4) Interactions with the Innate Immunity Receptor Complex

Sonia Podvin[1], **Xitong Dang**, **Morgan Meads**, **Arwa Kurabi**, **Todd Costantini**, **Brian P. Eliceiri**, **Andrew Baird**[*], and **Raul Coimbra**
Division of Trauma, Burns and Surgical Critical Care, Department of Surgery, University of California, San Diego, San Diego, California

Abstract

Objective and design—The human c2orf40 gene encodes a tumor suppressor gene called esophageal cancer-related gene-4 (ECRG4) with pro- and anti-inflammatory activities that depend on cell surface processing. Here, we investigated its physical and functional association with the innate immunity receptor complex.

Methods—Interactions between ECRG4 and the innate immunity receptor complex were assessed by flow cytometry, immunohistochemistry, confocal microscopy, co-immunoprecipitation. Phage display was used for ligand-targeting to cells that over express the TLR4-MD2-CD14.

Results—Immunoprecipitation and immunohistochemical studies demonstrate a physical interaction between ECRG4 and TLR4-MD2-CD14 on human granulocytes. Flow cytometry shows ECRG4 on the cell surface of a subset of $CD14^{+}$ and CD16+ leukocytes. In a cohort of trauma patients, the C-terminal 16 amino acid domain of ECRG4 ($ECRG4^{133–148}$), appears processed and shed, presumably at a thrombin-like consensus sequence. Phage targeting this putative ligand shows that this peptide sequence can internalizes into cells through the TLR4/CD14/MD2 complex but modulates inflammation through non-canonical, NFκB signal transduction.

Conclusions—ECRG4 is present on the surface of human monocytes and granulocytes. Its interaction with the human innate immunity receptor complex supports a role for cell surface activation of ECRG4 during inflammation and implicates this receptor in its mechanism of action.

Keywords

ECRG4; TLR4; CD14; MD2; innate immunity; phage; leukocyte

[*]**Corresponding author:** Andrew Baird, abaird@ucsd.edu, 619-4571-9027 (TEL), 619-543-2325 (FAX).
[1]Current address: Skaggs School of Pharmacy and Pharmaceutical Sciences, University of California San Diego, La Jolla, California, 92093

Author contributions: SP, XD and AK performed immunoprecipitation studies. SP prepared, qualified and tested peptide-targeted phage and developed quantitative phage recovery assay. BEP and MM collected, prepared and analyzed human volunteer blood by flow cytometry while TC and MM collected, prepared and analyzed human blood from trauma patients. BEP and AB performed the confocal microscopy from which RC and AB conceived of a physical TLR4-ECRG4 interaction. SP and AB wrote the first drafts of the manuscript with analytical, editorial and content assistance by BPE, TC and RC. Content was further edited and clarified by XD, MM and AK.

INTRODUCTION

In humans, the esophageal cancer-related gene-4 protein (ECRG4, NP_115787) is encoded by chromosome 2, open reading frame 40 (c2orf40, NM_032411.2). When the ECRG4 gene is expressed, c2orf40 produces a highly conserved, neuropeptide hormone-like 148 amino acid precursor protein [1] that is constitutively secreted [2, 3] and tethered to the cell surface until proteolytically processed [4, 3, 5]. Because of its down regulation in cancer [6–13], ECRG4 is presumed to act as a tumor suppressor but several studies point to it playing a constitutive inhibitory function in the normal regulation of immunosurveillance as well as epithelial and mesenchymal cell proliferation [14, 5, 15–18, 4, 19]. On one hand, the degree of its epigenetic silencing by hypermethylation and the decreased levels of C2orf40 gene expression are correlated with tumor growth, progression and metastasis of many types of epithelial cancers, such as esophageal, prostate and breast cancers and to several gliomas and CNS tumors [9, 8, 6, 10–13]. On the other hand, the products of c2orf40 (ECRG4) in normal tissues are associated with both anti- and pro-inflammatory activities that affect cell differentiation [15], senescence [16] and the proliferative responses to injury, inflammation and infection [4, 5] that seem to depend on its activation and processing [14].

In man, the physiological, let alone pathophysiological consequences of ECRG4 secretion and processing remain largely unknown. Yet, pro-inflammatory biological activities have been ascribed to small molecular weight peptides derived by processing of ECRG4 [15, 16, 2, 3] while anti-inflammatory activities ascribed to the intact cell surface precursor [5, 17, 18, 4, 19]. Recently however, human leukocytes and specifically, polymorphonuclear leukocytes (PMNs), have been identified as a particularly rich source of ECRG4 gene expression[5] and ECRG4 processing at the PMN cell surface has been suggested to contribute to the leukocyte response to inflammation, infection and injury[5]. To this end, ECRG4 co-localizes on the neutrophil surface with protein components of the innate immunity receptor complex which, like ECRG4 [5, 3, 20–22], are associated with infection, immunity and cancer [23–29]. In the studies reported here, we characterize a physical and biological link between ECRG4 and these components of the innate immunity receptor complex using cells that over express TLR4/CD14/MD2. We also demonstrate that a ECRG4 C-terminus peptide called CΔ16-ECRG4$^{133–148}$ is generated by thrombin-like processing of ECRG4 and biologically active.

MATERIALS AND METHODS

Antibodies

Affinity purified polyclonal antibodies raised against TLR4 (rabbit), CD14 (goat) and MD2 (rabbit) were acquired from Santa Cruz Biotech. In FACS studies, a polyclonal anti–ECRG4 IgY antibody was raised in chickens against ECRG4 (71–148) by commercial contract to GenWay Biotech (San Diego, CA). Antibodies used to detect the C-terminal region of ECRG4 in IP studies were a rabbit polyclonal antiserum (Ab-G) to ECRG4 raised by commercial contract to ProSci, Inc. (Poway, CA), an epitope specific antibody (Ab-P) recognizing the CΔ16 peptide ECRG4(133–148) was from Phoenix Pharmaceuticals (Burlingame, CA) and Ab-S, an affinity purified rabbit anti-C2orf40 purchased from Sigma-Aldrich (St. Louis, MO). Anti-rabbit AlexaFluor 488 and 594 secondary antibodies were

used for confocal microscopy (Life Technologies, Grand Island, NY) and mouse monoclonal antibodies to phage p3 coat protein or epidermal growth factor were purchased from Mo Bi Tec (Gottingen, Germany) and Sigma respectively.

Cell lines and assays for innate immunity receptor activation

HEK 293 cells stably overexpressing human TLR4, CD14 and MD2 (HEK-Blue-4™, InVivoGen, San Diego, CA) and TNFα/IL-1β (HEK-Blue™ TNF-α/IL-1β) were grown in DMEM growth media as above for parental HEK 293 cells but also containing the selection antibiotics blasticidin, hygromycin and zeocin™. The HEK-Blue-4 response to lipopolysaccharide (LPS, E coli Sigma L2654) was performed according to the manufacturer's recommended procedure. As indicated, the assay was performed in the presence of the indicated Δ16 peptide alone or in the presence of LPS.

Human peripheral leukocytes

The University of California San Diego Institutional Review Board approved study participants, protocols, and consent forms. Informed consent was obtained and blood samples were collected from 20 healthy volunteers (15 male, 5 female) aged 19 to 56 (median 30.5) and 9 trauma patients aged 5–36 (median 14) that presented after vehicle collision (N=5) or penetrating injury (N=5) and admitted to the University of California San Diego Burn Center between June 20113 and March 2014. All studies were performed with informed consent and prior approval of, and strict adherence to, guidelines set forth by the Institutional Review Board for Human Studies at the University of California, San Diego Medical Center (San Diego, CA). Patients were treated using modern trauma patient care protocols with aggressive fluid resuscitation, early enteral feeds and ventilator support as clinically indicated. Blood was collected from trauma patients with informed consent on the 4^{th} day after admission. In all cases, red blood cells were lysed with BD Pharm Lyse™ ammonium chloride solution (BD Biosciences, San Diego, CA), leukocytes pelleted by centrifugation and after washing with PBS processed immediately for flow cytometry or immunoprecipitation studies.

Flow cytometry analyses of human blood

Healthy human blood was collected in heparinized tubes and leukocytes harvested as above following ammonium chloride lysis of red blood cells for 15 minutes at room temperature (BD Pharm Lyse™, BD Biosciences). Cells were washed and fixed using Cytofix (BD Biosciences) for 10 minutes on ice. Cells were incubated in primary antibodies (1) anti-ECRG4 IgY (ECRG4-C) (2) mouse anti-CD16 APC-Cy5 conjugated clone M5E2 (BD Biosciences) (3) mouse anti-CD14 APC conjugated clone 3G8 (BD Biosciences) in FACs buffer (1% BSA in phosphate buffered saline (PBS) with 0.005% sodium azide) and washed in FACs buffer. Then, cells were incubated with the corresponding secondary antibodies (1) anti-chicken Alexa 488-conjugated (Life Technologies). Flow cytometry was performed with a Becton Dickinson FACSCalibur and data analysis performed with CellQuestPro software from Becton Dickinson.

Phagemid cloning

The ORF region corresponding to human ECRG4 CΔ16 peptide sequence (^{133}SPYGFRHGASVNYDDY^{148}) was placed directionally into the pIII ORF by cloning the sequence in the pUC198 M13 phagemid vector with 5' restriction enzyme BspH I and 3' Pst I restriction enzyme. The CΔ16 fragment was amplified from vector SC104814, which contains the human c2orf40 cDNA (Origene, Rockville, MD) using forward primer 5'-AAAATCATGAGCCCCTACGGCTTTAGCATGGAGCCAGC-3' and reverse primer. 5'-AAAACTGCAGAACCTCCTCCACCGTAGTCATCGTAGTTGACGCT-3.' Phagemid was transformed into XL1blue-MRF' cells (Agilent Technologies) and sequenced clones selected for phage preparation.

Phage preparation

XL1blue-MRF' *E. coli* (Agilent Technologies, Santa Clara, CA) was transformed with pUC198, pUC198-EGF or pUC198-CΔ16 phagemid and grown to OD_{600} = 0.15 in 2xYT broth (1.6% peptone, 1% yeast extract and 0.5% NaCl) with 2% glucose and 50 μg/ml ampicillin. Helperphage (Hyperphage M13K07ΔpIII, Fitzgerald Industries International, Acton, MA) was added at plasmid to cell ratio of 10:1 and incubated at 37°C for 1 hour. PIII replication and phage production was induced by incubating *E.coli* with 200 μM of IPTG overnight at 30°C. Phage was purified from bacterial debris by two rounds of incubation on ice with ¼ volume of polyethylene glycol (PEG) and centrifugation. Bacterial DNA was digested by incubation with $MgCl_2$, DNaseI and EDTA. Phage was then again purified by PEG precipitation. Finally, endotoxin was removed from phage preparations by incubating with 15% of Triton X-114 (Sigma) on ice for 30 min, then 37°C for 10 min as described previously [30]. Phage was pelleted by centrifugation for 10 min at room temperature. This process was repeated twice. Phage titer was determined by sandwich ELISA. Briefly, 96-well plates were coated with 5 μg/ml rabbit anti-fd antibody (Sigma) overnight. Plates were washed twice with PBS containing 0.05% Tween-20 (PBS/T) and blocked with 0.1% BSA in PBS/T for 1 hour at room temperatures. Blocking solution was washed 4 times with PBS/T. A phage prep of known concentration was used to create a standard curve of dilutions. New phage preparations were diluted successively 1:3 and incubated with primary antibody for 90 minutes at room temperature. Phage-antibody complexes were then washed 4 times in PBS/T and an HRP-conjugated mouse monoclonal antibody against M13 (R&S Systems, Minneapolis, MN) was diluted to 2 μg/ml in 0.1% BSA in PBS/T and incubated with antigen for 1 hour at room temperatures. The phage-antibody complexes were then washed in PBS/T 4 times. SigmaFast OPD (Sigma) was used as an HRP substrate according to manufacturer's instructions and incubated with the ELISA for 15 minutes at room temperature protected from light. The reaction was stopped with 25 μl/well of 3N HCl and the absorbance determined at 490 nm.

Quantification of internalized phage particles with quantitative PCR (qPCR)

Cells were plated at 500,000 cells/ml in untreated 6-well tissue culture plates and grown to confluence. Following incubation with phage diluted in complete DMEM, media was removed and cells treated with 0.25% trypsin-EDTA to detach from the tissue culture plate. Cells were washed 6 times in then received glycine/salt acid wash for 15 min at 37°C and

washed 3 more times in PBS. DNA was extracted from cells by (1) resuspension of cells in 320 µl 10 mM tris pH 8.5, 10 mM EDTA, 10% SDS and 20 µg/ml Proteinase K for 2 hours at 37°C; (2) addition of NaCl to 1.1 M final concentration and stored at 4°C overnight; (3) cells were pelleted and DNA phenol:chloroform extracted using a standard procedure; (4) DNA was precipitated with 3 M sodium acetate, 100% ethanol and glycogen. The DNA pellet was washed with 70% ethanol and resuspended in 5 µl of 10 mM tris-Cl, pH 8.5. One microliter was used as template for real-time qPCR amplification. The number of internalized phage particles relative to genomic GAPDH and fold change of HEK-TLR4/CD14/MD2 cells relative to HEK TNFαR/IL-1βR cells were determined using the ΔΔCt method. Reactions were run on an iQ5 Real-Time PCR machine (Bio-Rad, Hercules, CA) with SYBR green detection (iQ SYBR Green 2× master mix, Bio-Rad) with the following parameters: 10 min at 95°C; 45 × [95°C for 30 sec, 60°C for 30 sec, 72°C for 30 sec] 72°C for 2 min. For phagemid amplification the primers used were sense 5'-GGAAACAGTATGACCATGATTACGCC-3' and antisense 5'-CAGGTCAGACGATTGGCCTTGATATTCAC-3'. For amplification of genomic GAPDH exon 7 the primers were used were forward 5'-ACAGTCCATGCCATCACTGCCAC-3' and reverse 5'-AGGTCCACCACTGACACGTTGGC-3'. Each set of primers was diluted to 0.1 pmol/µl in each reaction. Efficiency of primers was determined to be 95–100% by standard curve, and melt curves were used to assure the correct amplicon size. Results shown in Figure 4 are representative of n=2 replicates of the experiment. Statistical significance was calculated by two-tailed Student's T-test, with significant difference defined as $p < 0.05$. The error bars shown in Figure 4 indicate the range of fold changes between untargeted and targeted phage.

Immunostaining of neutrophils for confocal microscopy

Unpermeabilized human PMNs were subjected to immunofluorescence staining following fixation in 2% paraformaldehyde in 2% glucose, 0.1 M sodium phosphate buffer, pH 7.2 for 20 minutes at room temperature. Cells were blocked with 5% normal donkey serum in 1% BSA for 30 minutes at room temperature. The affinity purified chicken anti-ECRG4 IgY antibody (Genway, 1:2000), and either rabbit polyclonal anti-TLR4 (sc-10741, Santa Cruz , 1:250), goat polyclonal anti-CD14 (sc-6998, Santa Cruz ,1:250), or rabbit polyclonal anti-MD2 (sc-20668, Santa Cruz ,1:250), diluted in 1% BSA/PBS and incubated for one hour at room temperature. Following further PBS wash, the appropriate Alexa-fluor-conjugated secondary antibodies (Molecular Probes, Eugene, OR, 1:700) were incubated for 1 hour at room temperature, washed in PBS, mounted in Slow fade for imaging and imaged with an Olympus Fluoview 1000 (ASW 1.7b) laser scanning confocal microscope (Olympus, Melville, NY).

Co-Immunoprecipitation and immunoblotting

Leukocytes from 2 ml of whole blood (see above) were lysed with RIPA buffer containing protease inhibitor cocktail (Pierce, Rockford, IL) and run through a 21 g needle. Insoluble material was pelleted at 10,000 × *g* and discarded. Soluble protein was pre-cleared with 2 µg of goat (for CD14) or rabbit (for TLR4 and MD2) normal IgG and protein A/G agarose (Santa Cruz Biotech) 1 hr at 4°C with rotation. IgG bound proteins were centrifuged at 2500 × *g* and discarded. Goat anti-CD14, rabbit anti-TLR4 and rabbit anti-MD2 (Santa Cruz

Biotech) were each added at 2 μg and incubated overnight at 4°C with rotation. The following day, 20 μl of protein A/G beads were added and incubated for 1 hour with rotation. Protein complexes were pelleted at 2500 × *g* and washed three times with RIPA buffer. Protein was eluted by boiling in reducing 1× lithium dodecyl sulfate sample buffer (Invitrogen) and centrifugation to pellet agarose beads. An immunoblotting protocol described previously was used [4], and primary antibody concentrations (0.1 μg/ml) were used for anti-ECRG4$^{(72–148)}$ prepared by Genway (Ab-G), anti recombinant ECRG4$^{(31–148)}$ by Sigma (Ab-S) or anti-ECRG4$^{(133–148)}$ purchased from Phoenix laboratories (Ab-P). The antibodies used to detect pIII phage coat protein and epidermal growth factor (EGF) were purchased from (Sigma) and used at a concentration of 0.01 μg/ml.

RESULTS

ECRG4 is present on the surface of human neutrophils

To demonstrate that ECRG4 localizes to surface of human granulocytes, we processed peripheral human blood leukocytes for immunostaining using anti-ECRG4 antibodies and analyzed the cell staining by flow cytometry (Figure 1). First, forward and side scatter parameters were used to gate granulocytes and monocytes (Figure 1A) and we observed that there were markedly higher levels of ECRG4 on the surface of neutrophils compared to monocytes (Figure 1B). We validated this staining pattern by co-staining ECRG4 stained cells with an anti-CD16 antibody that detects primarily neutrophils. In these experiments, we observed the presence of a nearly uniform population of ECRG4^{+}/CD16^{+} neutrophils (Figure 1C). Similar flow cytometry analysis with an anti-CD14 antibody established the existence of ECRG4^{+}/CD14^{+} monocytes but only about 10% of the CD14^{+} monocytes were also ECRG4^{+} (Figure 1D). Because these cells are non-permeabilized, these data are consistent with ECRG4 being a membrane-bound protein that is localized to the surface of leukocytes, widely expressed but most prominent on circulating human neutrophils then monocytes.

Neutrophil-derived Ecrg4 is processed at the cell surface in vivo

Previous studies have shown that upon neutrophil activation, ECRG4 sheds a C-terminus peptide fragment (CΔ16-ECRG4$^{133–148}$) that is generated by thrombin-like processing of ECRG4 on the cell surface [5]. As illustrated in Figure 2A, the processing of CΔ16-ECRG4$^{133–148}$ immunoreactivity on the cell surface can be detected using CΔ16-ECRG4$^{133–148}$ epitope-specific antibodies although he shed CΔ16-ECRG4$^{133–148}$ peptide could be detected by proteomic analyses of biological fluids including human serum, plasma cerebrospinal fluid and the media of cells over expressing ECRG4 [31, 32, 3].

To evaluate the possibility of ECRG4 processing *in vivo* (Figure 2), we used two antibodies in flow cytometry and assessed the nature of cell surface ECRG4 on leukocytes. In the analyses presented in Figure 2B-E, peripheral blood was analyzed from either 20 human volunteers or 9 trauma patients on their 4th day after admission to the UCSD Level 1 Trauma Center as described in materials and methods. We observed that approximately 5–10% of circulating CD14^{+} cells were ECRG4^{+} (Figure 2B) and 30–75% of CD16+ cells were ECRG4^{+} (Figure 2C). When we evaluated ECRG4 in the same healthy human donor

population using a second epitope-specific antibody that only recognizes the shed CΔ16-ECRG4$^{133–148}$ peptide we observed significant concordance in median cell surface ECRG4+ immunoreactivity Up to 80% of ECRG4^{+} of cells that stain for ECRG4 with one antibody also stain with the anti-ECRG4$^{133–148}$ antibodies in monocytes (Ratio in Figure 2B) and a median of 65% of granulocytes (Ratio in Figure 2C) that stain for ECRG4 with one antibody also stain with the anti-ECRG4$^{133–148}$. We interpret this finding to indicate that in processing blood from normal human volunteers, there some loss of CΔ16-ECRG4$^{133–148}$ but that the majority of ECRG4 on the cell surface is intact. We also observed that processing, storage time, and treating blood with thrombin significantly alters the CΔ16-ECRG4$^{133–148}$ to full length ECRG4 ratio (data not shown). Interestingly, we observed a significantly different detection of the CΔ16-ECRG4$^{133–148}$ to ECRG4 ratio on CD16^{+} cells when we examined blood from the cohort of 9 trauma patients that was processed exactly as volunteer blood. While the anti-ECRG4 antibody which recognizes the core extracellular 71–132 amino acids of ECRG4 detected up to 80% of CD16^{+} cells, antibodies to the Ecrg4$^{133–148}$ peptide detect less then 15% of cells in these same preparations (Figure 2C). The median ratio of CΔ16-ECRG4$^{133–148}$ to ECRG4 was 0.30 ($p<.001$) in trauma patients which was significantly different from that observed in healthy human volunteers (Figure 2D).

Co-localization of ECRG4 with TLR4 /MD2 and CD14 components of the LPS receptor complex on CD14^{+}/CD16^{+} leukocytes

Several lines of evidence led us to suspect that TLR4 and the innate immunity receptor complex might interact with ECRG4 on the leukocyte cell surface. First, ECRG4 is present on subpopulations of leukocytes that are LPS responsive (Figure 1) including CD14, an integral member of the innate immunity receptor [33] that is present on human neutrophils [34]. Second, we had previously used immunohistochemistry to show that ECRG4 co-localized with MD2, TLR4 and CD14 on leukocytes [5]. Finally, a treatment of peritoneal macrophages with CΔ16-ECRG4$^{133–148}$ increased phosphorylated NF-κB expression [5], a canonical pro-inflammatory response to LPS receptor complex activation.

We used two techniques to study a possible interaction between ECRG4 and the innate immunity receptor complex. First, we used confocal microscopy to assess cell surface co-staining of fixed, unpermeabilized human granulocytes (PMNs) that had been isolated by Ficoll centrifugation (Figure 3A), Second, we used co-immunoprecipitation of ECRG4 with antibodies to TLR4, CD14 and MD2 (Figure 3B). In immunohistochemistry studies, antibodies that detected each of the three main components of the TLR4 receptor complex (left panels, red), closely co-localized with the co-staining obtained with an antibody to ECRG4 (middle panels, green). Merging the innate immunity receptor (in red) and ECRG4 (in green) signals suggested close physical proximity and co-localization (right panels, yellow) in what appears to be non-homogeneous patterns like those reported for lipid rafts [34].

Biophysical evidence for an interaction between ECRG4 and the innate immunity receptor was obtained by co-immunoprecipitation. Freshly harvested human PMNs were lysed and the three main components of the innate immunity receptor, TLR4, CD14 and MD2 were

immuno-precipitated as described in Materials and Methods. Three different antibodies (ab-i, abii and ab-iii) that were raised against three different preparations of human ECRG4 were used to immunoblot the immuno-precipitates and each detected the same 8–10 kDa ECRG4 peptide (Figure 3B). Because one antibody (Ab-P) was raised against the CΔ16-ECRG4$^{(133–148)}$ peptide, the results identify the C-terminus of ECRG4 as the interacting domain. No ECRG4 immunoreactivity was observed in control immuno-precipitates (Figure 3B, left lanes of each panel). Taken together, the data suggest that the co-localization and physical proximity of the C-terminal of ECRG4 with the TLR4 innate immunity receptor complex is mediated by a molecular interaction that involves the C-terminus of ECRG4.

Cells expressing TLR4, CD14, and MD2 bind and internalize CΔ16-targeted phage

To test the hypothesis that the C-terminal domain of ECRG4 interacts with the TLR4 innate immunity receptor complex, we exploited the ability of ligands to retarget viral particles to bind and internalize into mammalian cells [35, 30, 36, 37]. As shown in Figure 4, bacteriophage that are genetically engineered to display the C-terminus CΔ16-ECRG4$^{133–148}$ peptide bind and internalize into cells engineered to overexpress the TLR4 innate immunity receptor complex but not into cells engineered to overexpress the TNF/IL1 receptor.

HEK-Blue-4™ cells are a human embryonic kidney-derived cell line that stably overexpresses the subunits of the innate immunity receptor complex including TLR4, CD14 and MD2 [38–40]. We therefore hypothesized that M13 phage, reengineered to display the CΔ16-ECRG4$^{(133–148)}$ peptide would bind to, and internalize through, the overexpressed innate immunity receptor complex at levels that are significantly higher than control HEK293 cells which express low endogenous levels of these proteins [41–43].

Phage displaying the CΔ16-ECRG4$^{133–148}$ peptide was prepared as described in Materials and Methods. EGF-targeted phage was used to verify receptor-mediated endocytosis knowing that HEK cells express endogenous high affinity EGF receptors [44, 45]. To prove the authenticity of the re-engineered phage, lysates were immunoblotted with antibodies to phage plll protein (Figure 3A left panels) or to the appropriate ligand (EGF or CΔ16 ligands, right panels). As expected, the display of EGF-plll as a fusion protein shows plll immunoreactivity at the expected higher 38 kDa (arrow). Immunoblotting the CΔ16-ECRG4$^{133–148}$ peptide on phage shows a similar MW and the display of the CΔ16 peptide is confirmed by immunoblotting with an anti-ECRG4$^{(133–148)}$ specific antibody but not WT phage. (Figure 4A, bottom right panel, arrow).

To control for any non-specific effects of transfection, stable transduction and protein over expression ligand targeting was evaluated in HEK-blue reporter cells that overexpress the TNFα and IL-1β receptor (TNFR/IL1βR). WT phage, EGF-phage and CΔ16-phage were added to both HEK-TLR4/CD14/MD2 and HEK-TNFR/IL-1βR cells and qPCR used to quantify the amount of particle internalization. Cell surfaces were washed with high salt and at low pH to remove all phage that non-specifically bound to the cell surface and did not internalize. Phage DNA was extracted from cell lysates and the levels of internalized phage analyzed by qPCR in HEK-TLR4/CD14/MD2 (Figure 4B) or control HEK-TNFR/IL1βR (Figure 4C) cells. Both cell lines internalized some WT phage non specifically and, because

HEK cells express high affinity EGF receptors [46], both cell types internalized EGF-phage (Figure 4B and 4C middle bars). In contrast, the amounts CΔ16-ECRG4$^{133–148}$ peptide targeted phage DNA that was recovered from HEK-TLR4/CD14/MD2 cells was approximately 5–7 fold higher than that of wild-type phage (Figure 4B right bar) and there was no internalization in HEK-TNFR/IL-1βR cells (Figure 4C right bar). As predicted, there was no difference in the ability of cells to internalize EGF-phage. These data support the hypothesis that the TLR4 innate immunity receptor is a cell-surface binding complex that interacts with and can internalize the CΔ16 peptide domain of ECRG4.

To determine whether binding and internalization was sufficient for cell signaling, the TLR4 overexpressing HEKblue cells were treated with the CΔ16-ECRG4$^{133–148}$ peptide in the presence or absence of LPS (Figure 4D). No differences were observed in cell responsiveness despite the fact that the same Δ16-ECRG4$^{133–148}$ peptide can activate mouse peritoneal macrophages [5] and increase the expansion of mucosal epithelial cell explants in vitro (not shown).

DISCUSSION

The findings presented here show that ECRG4 is expressed on the surface of up to 10% of CD14^{+} monocytes and 75% of human CD16+ neutrophils (Figure 1). We also find that proteolytic processing during/after injury likely releases a 16 amino acid C-terminus ECRG4$^{133–148}$ peptide that can skew the detection of ECRG4 with certain anti-ECRG4 antibodies (Figure 2). This proteolytic shedding most likely occurs at a putative thrombin-like consensus cleavage sequence that releases a CΔ16 ECRG4$^{133–148}$ pro-inflammatory peptide [5] that has been detected by proteomic analyses in plasma, serum, cerebrospinal fluid and the conditioned media of ECRG4 over expressing cells[31, 32, 3]. We also show that the ECRG4 protein on the surface of neutrophils physically interacts with the innate immunity receptor complex on the cell surface (Figure 3) and that a processed C-terminus ECRG4$^{133–148}$ peptide can specifically use the TLR4 innate immunity receptor complex to enter cells (Figure 4). These data point to involvement of the innate immunity receptor complex in the dual pro- and anti-inflammatory activities ascribed to different peptides processed from ECRG4 precursor [14].

Among circulating ECRG4^{+} leukocytes, a greater percentage of cells are CD16+ granulocytes rather than CD14^{+} monocytes (Figure 1). This makes CD16+ granulocytes the more likely source of extracellular CΔ16 peptide found in human biological fluids, although the contribution of ECRG4 expressed in epithelial cells [14] remains unknown. Neutrophils however play a major physiological function in coordinating the recruitment of monocytes after injury and they assist in the transition of macrophage function towards phagocytosis [47]. Their release of CΔ16 ECRG4$^{133–148}$ is likely derived from shedding ECRG4 from the cell surface rather then release from neutrophil granules [48], although the latter cannot be excluded. Because the shedding of tethered precursor-derived peptides in response to both injury and infection has been well described for numerous other cell surface proteins [49–51], the findings reported here are consistent with the hypothesis that a full-length cell surface tethered ECRG4 is activated at the cell surface to release the CΔ16 peptide (Figure 5).

Both the higher molecular weight cell surface ECRG4 protein and its processed CΔ16 peptide appear to interact with the TLR4 innate immunity receptor complex. On one hand, these findings establish the physical proximity between, and biochemical interaction with ECRG4 and the TLR4 innate immunity receptor complex (Figure 3). The interaction was detected by immunoblotting immuno-precipitates of the TLR4 innate immunity complex with three different ECRG4 antibodies and the findings are compatible with the reported distribution and activities of both ECRG4 and the innate immunity receptor complex in injury response [52–59, 48, 60]. In this paradigm, a membrane tethered ECRG4 precursor may play a surveillance inhibitory function on circulating PMNs [5] and epithelial cells [17] that helps gauge responsiveness and specialized barrier function [14].

Cell surface processing of ECRG4 by proteases activated during the injury and inflammation responses can generate several smaller peptides that are of unknown physiological significance [3, 2, 14]. The 16 amino acid C-terminus CΔ16 ECRG4$^{133–148}$ peptide is one that we show here can specifically enter cells that overexpress the TLR4 innate immunity receptor complex. Interestingly, we failed to detect NF-Kb activation in this reporter line suggesting that either it activates non-canonical pathways in mouse peritoneal macrophages [5] or that there is a heretofore unidentified component to the innate immunity receptor that is responsible for Δ16-ECRG4$^{133–148}$ peptide signaling. Additionally, internalization may be an activity that is shared by all ECRG4 peptides that contain the CΔ16 ECRG4$^{133–148}$ sequence (Figure 5). In this paradigm, the CΔ16 ECRG4$^{133–148}$ peptide could be a minimally active biological core that is required for ECRG4 interactions with the innate immunity receptor complex interactions, its binding and internalization. Alternatively, specific thrombin-like processing of cell surface ECRG4 during injury would generate a CΔ16 ECRG4$^{133–148}$ peptide that in turn could internalize into cells via the TLR4 innate immunity receptor complex. In this latter case, the interaction of a tethered ECRG4 to the TLR4 innate immunity receptor complex as established by co-immunoprecipitation and immunohistochemistry (Figure 2) could have significantly different activities than the processed and internalized CΔ16 ECRG4$^{133–148}$ sequence that is released by thrombin-like proteases. Interestingly, this could explain the observations that ECRG4 can have both pro- and anti-inflammatory activities and an ability to normally gauge cell growth and differentiation and the responsiveness to infection, injury, inflammation and malignancy.

ACKNOWLEDGEMENTS

The authors are indebted to Tran Nguyen, Emelie Amburn and Alexandra Ortiz-Borboa for expert technical assistance. Research was supported by a Mentored Young Investigator Award from the Hydrocephalus Association (S.P.), the National Institutes of Health through a P20 Exploratory Center grant for Wound Healing Research from the NIGMS (P20-GM078421) to X.D, A.B., B.E., and R.C. and from grants EY018479 (A.B.), DK085871 (A.B.), and HL73396 (B.P.E.) and supplemental funding by the National Eye Institute (NEI) and NIGMS through the American Recovery Act (ARRA). Studies with human blood were funded by a grant from the American Burn Association (RC)

References

1. Mirabeau O, Perlas E, Severini C, Audero E, Gascuel O, Possenti R, et al. Identification of novel peptide hormones in the human proteome by hidden Markov model screening. Genome Res. 2007; 17(3):320–327. [PubMed: 17284679]

2. Ozawa A, Lick AN, Lindberg I. Processing of proaugurin is required to suppress proliferation of tumor cell lines. Mol Endocrinol. 2011; 25(5):776–784. [PubMed: 21436262]

3. Dang X, Podvin S, Coimbra R, Eliceiri B, Baird A. Cell-specific processing and release of the hormone-like precursor and candidate tumor suppressor gene product, Ecrg4. Cell Tissue Res. 2012; 348(3):505–514. [PubMed: 22526622]

4. Podvin S, Gonzalez AM, Miller MC, Dang X, Botfield H, Donahue JE, et al. Esophageal cancer related gene-4 is a choroid plexus-derived injury response gene: evidence for a biphasic response in early and late brain injury. PLoS One. 2011; 6(9):e24609. [PubMed: 21935431]

5. Baird A, Coimbra R, Dang X, Lopez N, Lee J, Krzyzaniak M, et al. Cell surface localization and release of the candidate tumor suppressor Ecrg4 from polymorphonuclear cells and monocytes activate macrophages. J Leukoc Biol. 2012; 91(5):773–781. [PubMed: 22396620]

6. Su T, Liu H, Lu S. Cloning and identification of cDNA fragments related to human esophageal cancer. Zhonghua Zhong Liu Za Zhi. 1998; 20(4):254–257. [PubMed: 10920976]

7. Matsuzaki J, Torigoe T, Hirohashi Y, Tamura Y, Asanuma H, Nakazawa E, et al. Expression of ECRG4 is associated with lower proliferative potential of esophageal cancer cells. Pathology international. 2013; 63(8):391–397. [PubMed: 23957914]

8. Mori Y, Ishiguro H, Kuwabara Y, Kimura M, Mitsui A, Kurehara H, et al. Expression of ECRG4 is an independent prognostic factor for poor survival in patients with esophageal squamous cell carcinoma. Oncol Rep. 2007; 18(4):981–985. [PubMed: 17786363]

9. Yue CM, Deng DJ, Bi MX, Guo LP, Lu SH. Expression of ECRG4, a novel esophageal cancer-related gene, downregulated by CpG island hypermethylation in human esophageal squamous cell carcinoma. World J Gastroenterol. 2003; 9(6):1174–1178. [PubMed: 12800218]

10. Wang YB, Ba CF. Promoter methylation of esophageal cancer-related gene 4 in gastric cancer tissue and its clinical significance. Hepato-gastroenterology. 2012; 59(118):1696–1698. [PubMed: 22626786]

11. Li W, Liu X, Zhang B, Qi D, Zhang L, Jin Y, et al. Overexpression of candidate tumor suppressor ECRG4 inhibits Gliomas proliferation and invasion. J Exp Clin Cancer Res. 2010; 29(1):89. [PubMed: 20598162]

12. Vanaja DK, Ehrich M, Van den Boom D, Cheville JC, Karnes RJ, Tindall DJ, et al. Hypermethylation of genes for diagnosis and risk stratification of prostate cancer. Cancer Invest. 2009; 27(5):549–560. [PubMed: 19229700]

13. Donahue, JEMM.; Podvin, S.; Jackson, CL.; Johanson, CE.; Stopa, E.; Baird, A. Ecrg4 in normal and neoplastic choroid plexus. Presented at Society for Research into Hydrocephalus and Spina Bifida; Vancouver, BC, Canada. 2010.

14. Baird A, Lee J, Podvin S, Kuarbi A, Dang X, Coimbra R, et al. Esophageal-Cancer-Related Gene-4 (ECRG4) at the Interface of Injury, Inflammation, Infection and Malignancy. Gastrointestinal Cancer: Targets and Therapy. 2014 in press.

15. Huh YH, Ryu JH, Shin S, Lee DU, Yang S, Oh KS, et al. Esophageal cancer related gene 4 (ECRG4) is a marker of articular chondrocyte differentiation and cartilage destruction. Gene. 2009; 448(1):7–15. [PubMed: 19735703]

16. Kujuro Y, Suzuki N, Kondo T. Esophageal cancer-related gene 4 is a secreted inducer of cell senescence expressed by aged CNS precursor cells. Proc Natl Acad Sci U S A. 2010; 107(18): 8259–8264. [PubMed: 20404145]

17. Kurabi A, Pak K, Dang X, Coimbra R, Eliceiri BP, Ryan AF, et al. Ecrg4 attenuates the inflammatory proliferative response of mucosal epithelial cells to infection. PLoS One. 2013; 8(4):e61394. [PubMed: 23626679]

18. Shaterian A, Kao S, Chen L, DiPietro LA, Coimbra R, Eliceiri BP, et al. The candidate tumor suppressor gene Ecrg4 as a wound terminating factor in cutaneous injury. Archives of dermatological research. 2013; 305(2):141–149. [PubMed: 22899245]

19. Gonzalez AM, Podvin S, Lin SY, Miller MC, Botfield H, Leadbeater WE, et al. Ecrg4 expression and its product augurin in the choroid plexus: impact on fetal brain development, cerebrospinal fluid homeostasis and neuroprogenitor cell response to CNS injury. Fluids Barriers CNS. 2011; 8(1):6. [PubMed: 21349154]

20. Li LW, Yu XY, Yang Y, Zhang CP, Guo LP, Lu SH. Expression of esophageal cancer related gene 4 (ECRG4), a novel tumor suppressor gene, in esophageal cancer and its inhibitory effect on the tumor growth in vitro and in vivo. Int J Cancer. 2009; 125(7):1505–1513. [PubMed: 19521989]
21. Sabatier R, Finetti P, Adelaide J, Guille A, Borg JP, Chaffanet M, et al. Down-regulation of ECRG4, a candidate tumor suppressor gene, in human breast cancer. PLoS One. 2011; 6(11):e27656. [PubMed: 22110708]
22. Xu T, Xiao D, Zhang X. ECRG4 inhibits growth and invasiveness of squamous cell carcinoma of the head and neck and. Oncology letters. 2013; 5(6):1921–1926. [PubMed: 23833667]
23. Balistreri CR, Colonna-Romano G, Lio D, Candore G, Caruso C. TLR4 polymorphisms and ageing: implications for the pathophysiology of age-related diseases. Journal of clinical immunology. 2009; 29(4):406–415. [PubMed: 19459036]
24. Zhang K, Zhou B, Wang Y, Rao L, Zhang L. The TLR4 gene polymorphisms and susceptibility to cancer: a systematic review and meta-analysis. Eur J Cancer. 2013; 49(4):946–954. [PubMed: 23084080]
25. Wolska A, Lech-Maranda E, Robak T. Toll-like receptors and their role in carcinogenesis and anti-tumor treatment. Cellular & molecular biology letters. 2009; 14(2):248–272. [PubMed: 19096763]
26. Koller B, Bals R, Roos D, Korting HC, Griese M, Hartl D. Innate immune receptors on neutrophils and their role in chronic lung disease. European journal of clinical investigation. 2009; 39(7):535–547. [PubMed: 19453653]
27. Rallabhandi P, Bell J, Boukhvalova MS, Medvedev A, Lorenz E, Arditi M, et al. Analysis of TLR4 polymorphic variants: new insights into TLR4/MD-2/CD14 stoichiometry, structure, and signaling. J Immunol. 2006; 177(1):322–332. [PubMed: 16785528]
28. Huang B, Zhao J, Li H, He KL, Chen Y, Chen SH, et al. Toll-like receptors on tumor cells facilitate evasion of immune surveillance. Cancer Res. 2005; 65(12):5009–5014. [PubMed: 15958541]
29. Hua D, Liu MY, Cheng ZD, Qin XJ, Zhang HM, Chen Y, et al. Small interfering RNA-directed targeting of Toll-like receptor 4 inhibits human prostate cancer cell invasion, survival, and tumorigenicity. Molecular immunology. 2009; 46(15):2876–2884. [PubMed: 19643479]
30. Larocca D, Burg MA, Jensen-Pergakes K, Ravey EP, Gonzalez AM, Baird A. Evolving phage vectors for cell targeted gene delivery. Curr Pharm Biotechnol. 2002; 3(1):45–57. [PubMed: 11883506]
31. Holtta M, Zetterberg H, Mirgorodskaya E, Mattsson N, Blennow K, Gobom J. Peptidome analysis of cerebrospinal fluid by LC-MALDI MS. PLoS One. 2012; 7(8):e42555. [PubMed: 22880031]
32. Chank C, DM H, C S. Clinical proteomics analysis of the human serum proteome. NCI Large Human Serum Survey. 2012
33. Calvano JE, Agnese DM, Um JY, Goshima M, Singhal R, Coyle SM, et al. Modulation of the lipopolysaccharide receptor complex (CD14, TLR4, MD-2) and toll-like receptor 2 in systemic inflammatory response syndrome-positive patients with and without infection: relationship to tolerance. Shock. 2003; 20(5):415–419. [PubMed: 14560104]
34. Antal-Szalmas P, Strijp JA, Weersink AJ, Verhoef J, Van Kessel KP. Quantitation of surface CD14 on human monocytes and neutrophils. J Leukoc Biol. 1997; 61(6):721–728. [PubMed: 9201263]
35. Burg MA, Jensen-Pergakes K, Gonzalez AM, Ravey P, Baird A, Larocca D. Enhanced phagemid particle gene transfer in camptothecin-treated carcinoma cells. Cancer Res. 2002; 62(4):977–981. [PubMed: 11861367]
36. Larocca D, Jensen-Pergakes K, Burg MA, Baird A. Gene transfer using targeted filamentous bacteriophage. Methods Mol Biol. 2002; 185:393–401. [PubMed: 11769003]
37. Larocca D, Jensen-Pergakes K, Burg MA, Baird A. Receptor-targeted gene delivery using multivalent phagemid particles. Mol Ther. 2001; 3(4):476–484. [PubMed: 11319907]
38. Satta N, Kruithof EK, Fickentscher C, Dunoyer-Geindre S, Boehlen F, Reber G, et al. Toll-like receptor 2 mediates the activation of human monocytes and endothelial cells by antiphospholipid antibodies. Blood. 2011; 117(20):5523–5531. [PubMed: 21330474]

39. Naka T, Nakata N, Maeda S, Yamamoto R, Doe M, Mizuno S, et al. Structure and host recognition of serotype 13 glycopeptidolipid from Mycobacterium intracellulare. Journal of bacteriology. 2011; 193(20):5766–5774. [PubMed: 21856857]
40. Xu J, Zhang X, Monestier M, Esmon NL, Esmon CT. Extracellular histones are mediators of death through TLR2 and TLR4 in mouse fatal liver injury. J Immunol. 2011; 187(5):2626–2631. [PubMed: 21784973]
41. Yang H, Young DW, Gusovsky F, Chow JC. Cellular events mediated by lipopolysaccharide-stimulated toll-like receptor 4. MD-2 is required for activation of mitogen-activated protein kinases and Elk-1. J Biol Chem. 2000; 275(27):20861–20866. [PubMed: 10877845]
42. Espevik T, Latz E, Lien E, Monks B, Golenbock DT. Cell distributions and functions of Toll-like receptor 4 studied by fluorescent gene constructs. Scandinavian journal of infectious diseases. 2003; 35(9):660–664. [PubMed: 14620151]
43. Chow JC, Young DW, Golenbock DT, Christ WJ, Gusovsky F. Toll-like receptor-4 mediates lipopolysaccharide-induced signal transduction. J Biol Chem. 1999; 274(16):10689–10692. [PubMed: 10196138]
44. Kramer HK, Onoprishvili I, Andria ML, Hanna K, Sheinkman K, Haddad LB, et al. Delta opioid activation of the mitogen-activated protein kinase cascade does not require transphosphorylation of receptor tyrosine kinases. BMC pharmacology. 2002; 2:5. [PubMed: 11897012]
45. Shah BH, Neithardt A, Chu DB, Shah FB, Catt KJ. Role of EGF receptor transactivation in phosphoinositide 3-kinase-dependent activation of MAP kinase by GPCRs. J Cell Physiol. 2006; 206(1):47–57. [PubMed: 15920762]
46. Derrien A, Druey KM. RGS16 function is regulated by epidermal growth factor receptor-mediated tyrosine phosphorylation. J Biol Chem. 2001; 276(51):48532–48538. [PubMed: 11602604]
47. Soehnlein O, Lindbom L, Weber C. Mechanisms underlying neutrophil-mediated monocyte recruitment. Blood. 2009; 114(21):4613–4623. [PubMed: 19696199]
48. Kumar V, Sharma A. Neutrophils: Cinderella of innate immune system. International immunopharmacology. 2010; 10(11):1325–1334. [PubMed: 20828640]
49. Lederer JA, Brownstein BH, Lopez MC, Macmillan S, Delisle AJ, Macconmara MP, et al. Comparison of longitudinal leukocyte gene expression after burn injury or trauma-hemorrhage in mice. Physiological genomics. 2008; 32(3):299–310. [PubMed: 17986522]
50. Pillay J, Ramakers BP, Kamp VM, Loi AL, Lam SW, Hietbrink F, et al. Functional heterogeneity and differential priming of circulating neutrophils in human experimental endotoxemia. J Leukoc Biol. 2010; 88(1):211–220. [PubMed: 20400675]
51. Kopydlowski KM, Salkowski CA, Cody MJ, van Rooijen N, Major J, Hamilton TA, et al. Regulation of macrophage chemokine expression by lipopolysaccharide in vitro and in vivo. J Immunol. 1999; 163(3):1537–1544. [PubMed: 10415057]
52. Romero CD, Varma TK, Hobbs JB, Reyes A, Driver B, Sherwood ER. The Toll-like receptor 4 agonist monophosphoryl lipid a augments innate host resistance to systemic bacterial infection. Infect Immun. 2011; 79(9):3576–3587. [PubMed: 21646453]
53. Guha M, Mackman N. LPS induction of gene expression in human monocytes. Cellular signalling. 2001; 13(2):85–94. [PubMed: 11257452]
54. Xia Y, Yamagata K, Krukoff TL. Differential expression of the CD14/TLR4 complex and inflammatory signaling molecules following i.c.v. administration of LPS. Brain Res. 2006; 1095(1):85–95. [PubMed: 16697357]
55. Ye Y, Xu H, Zhang X, Li Z, Jia Y, He X, et al. Association between Toll-Like Receptor 4 Expression and Neural Stem Cell Proliferation in the Hippocampus Following Traumatic Brain Injury in Mice. International journal of molecular sciences. 2014; 15(7):12651–12664. [PubMed: 25036030]
56. Chakravarty S, Herkenham M. Toll-like receptor 4 on nonhematopoietic cells sustains CNS inflammation during endotoxemia, independent of systemic cytokines. J Neurosci. 2005; 25(7): 1788–1796. [PubMed: 15716415]
57. Wang J, Hori K, Ding J, Huang Y, Kwan P, Ladak A, et al. Toll-like receptors expressed by dermal fibroblasts contribute to hypertrophic scarring. J Cell Physiol. 2011; 226(5):1265–1273. [PubMed: 20945369]

58. Trinchieri G, Sher A. Cooperation of Toll-like receptor signals in innate immune defence. Nat Rev Immunol. 2007; 7(3):179–190. [PubMed: 17318230]

59. Fu Y, Glaros T, Zhu M, Wang P, Wu Z, Tyson JJ, et al. Network Topologies and Dynamics Leading to Endotoxin Tolerance and Priming in Innate Immune Cells. PLoS Comput Biol. 2012; 8(5):e1002526. [PubMed: 22615556]

60. Glezer I, Lapointe A, Rivest S. Innate immunity triggers oligodendrocyte progenitor reactivity and confines damages to brain injuries. FASEB J. 2006; 20(6):750–752. [PubMed: 16464958]

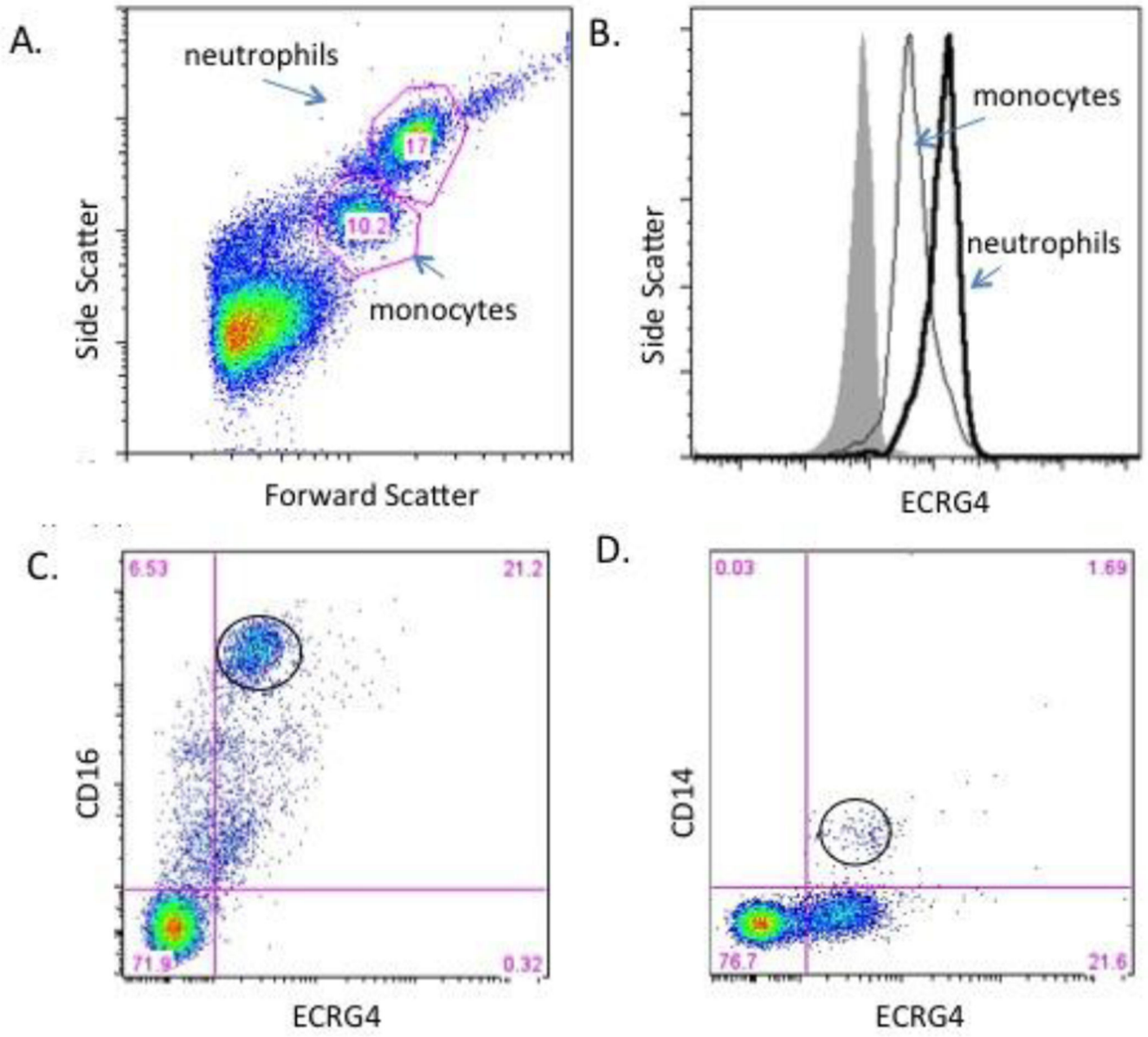

Figure 1. ECRG4 is present on the surface of CD16+, CD14+ and CD16+/CD14+ leukocytes

Panel A: FACs analysis of unpermeabilized human leukocytes shows two distinct populations of ECRG4+ cells that correspond to monocytes (middle grouping) and neutrophils (right grouping).

Panel B: Neutrophils (right peak, thick line) further indicate more ECRG4+ immunoreactive cells than monocytes (middle peak, thin line).

Panel C: Among CD16+ leukocytes, a standard marker of granulocytes, cell surface expression of ECRG4 in approximately 20–50% of cells (circle).

Panel D: among these CD16+ cells, 1–5% which are CD14+ express ECRG4. This indicates that a subset of leukocytes that are CD16+/CD14+/ECRG4+ and may correspond to Polymorphonuclear Neutrophils (PMNs).

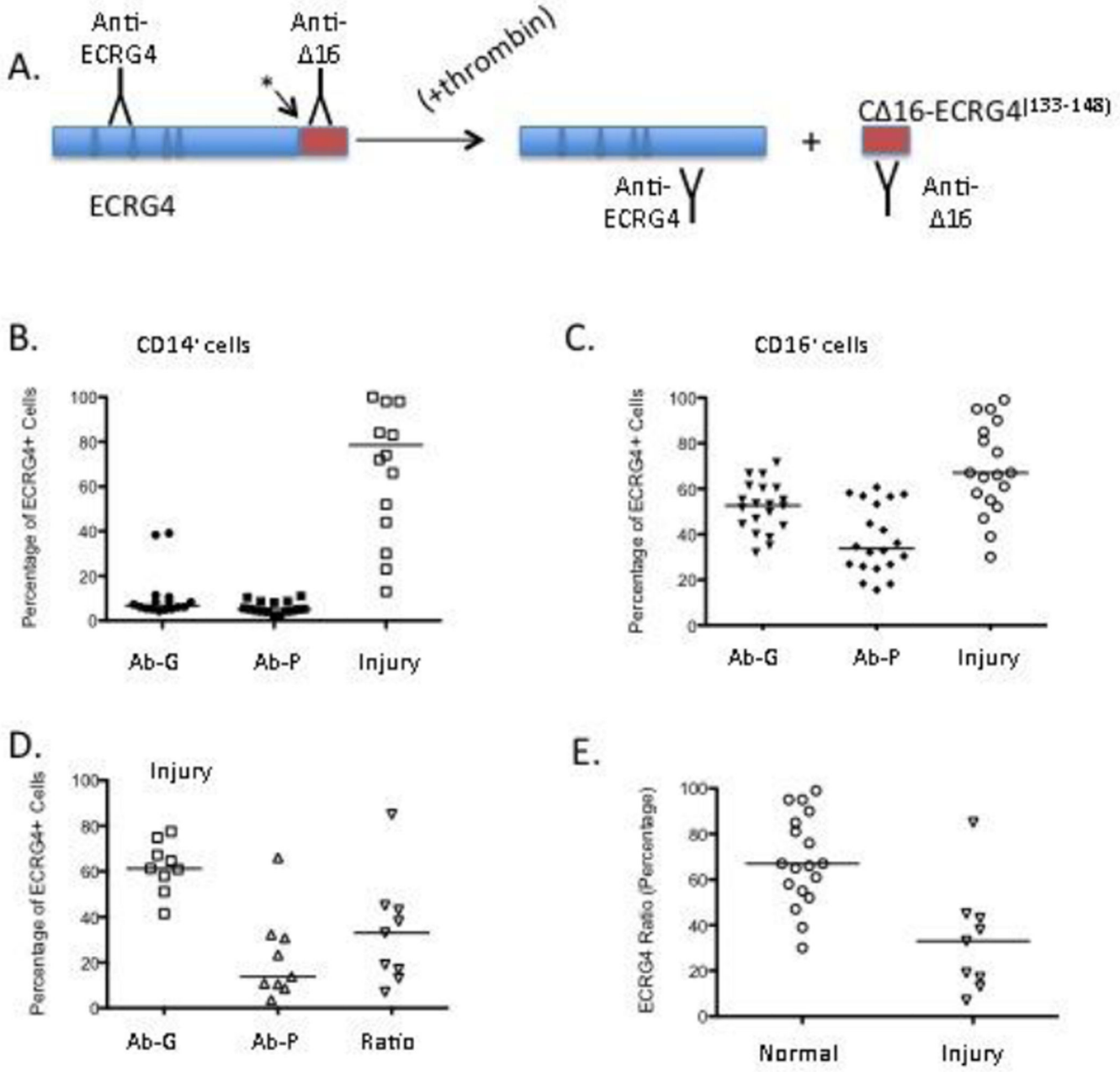

Figure 2. Evidence that neutrophil-derived ECRG4 is processed at the cell surface to release the CΔ16 peptide in vivo

Panel A: The G and P anti-ECRG4 antibodies were raised against either a recombinant ECRG4 (G) or a synthetic CΔ16-ECRG4$^{(133–148)}$ peptide (P). Both recognize ECRG4 on the cell surface, but if the ECRG4 is processed by thrombin-like cleavage, the CΔ16 ECRG4(133–148) peptide is released and staining with the P antibody is lost.

Panel B: Flow cytometry analyses of ECRG4 staining in CD14+ cells from normal volunteers shows low abundance (−10%) of ECRG4 using either the G antibody to intact ECRG4 or the P antibody raised against the CΔ16 ECRG4(133–148) peptide. Median

concordance of the flow cytometry for the ratio of CΔ16 ECRG4(133–148) to intact ECRG4 is 0.8.

Panel C: Flow cytometry analyses of ECRG4 staining in CD16+ cells from normal volunteers confirms the high abundance (−60%) of ECRG4 on granulocytes. Median concordance of the ratio of CΔ16 ECRG4(133–148) to intact ECRG4 is 0.7.

Panel D: In a cohort of trauma patients, flow cytometry analyses of ECRG4 staining in CD16+ cells in normal volunteers confirms the high abundance(−60%) seen in volunteers but staining with the P antibody is decreased and median concordance of the staining ratio of CΔ16 ECRG4$^{(133–148)}$ to intact ECRG4 is 0.35

Panel E: Compared concordance ratio in normal volunteers is 0.8 but decreased to 0.35 in trauma patients (P<.001).

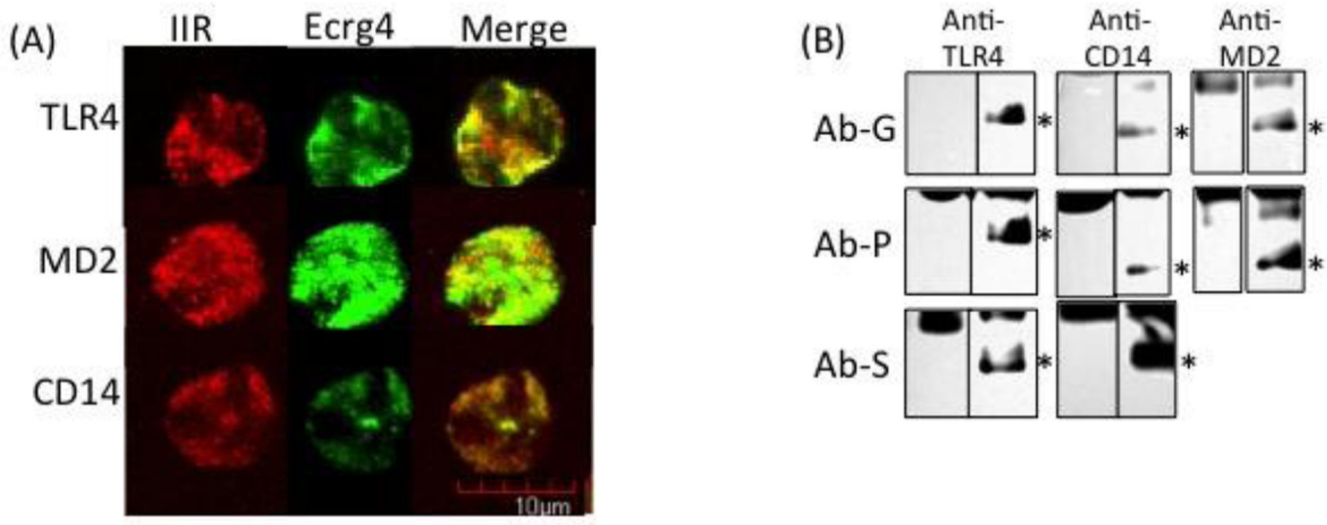

Figure 3. ECRG4 interacts with the TLR4, CD14 and MD2 subunits of LPS receptor complex

Panel A: Confocal microscopy of the cell surface of a human granulocyte following immunostaining for TLR4, CD14 orMD2 (red, left panels), and ECRG4 (green, middle panels) suggest co-localization which is supported by merged yellow signaling (red + green) in the right handed panels).

Panel B: An 8–10 kDa ECRG4 was detected in immunoprecipitated lysates of granulocytes by immunoblotting with three different antibodies to ECRG4 (Ab-G, Ab-P, Ab-S) as denoted by the asterix. Granulocyte immuno-precipitates were generated with antibodies to either TLR4, CD14 or MD2 as described in the text.

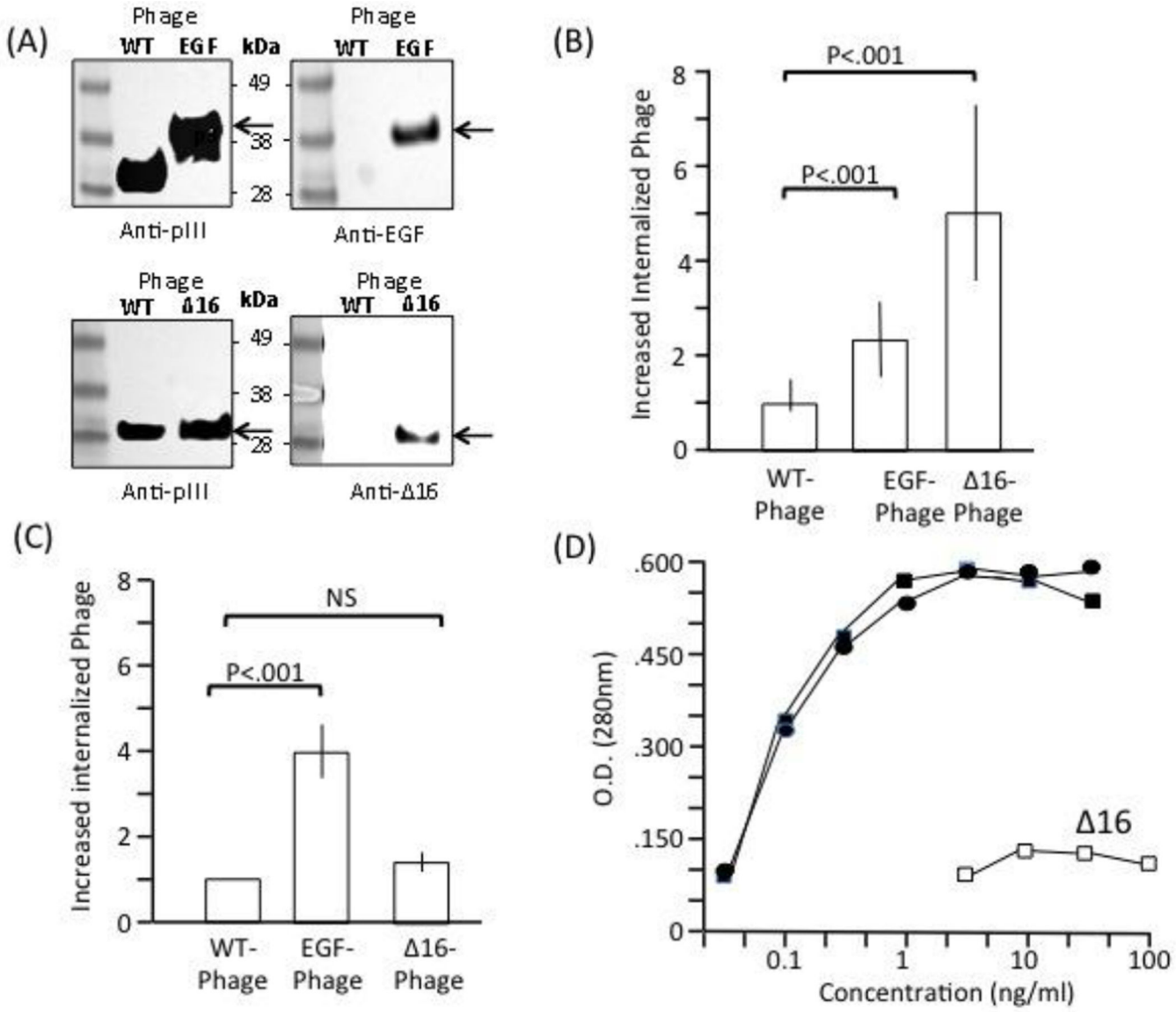

Figure 4. The ECRG4$^{(133–148)}$ domain binds the innate immunity receptor complex

Panel A: Immunoblotting confirms display of EGF and CΔ16-ECRG4$^{(133–148)}$ on M13 phage. Anti-pIII antibody detects WT phage, EGF-phage and the ΔC16-phage at the predicted 28 kDa MW (left panels). EGF is only detected in EGF phage (right panel, top). and ECRG4 detected in CΔ16-ECRG4$^{(133–148)}$ phage (right panel, bottom).

Panel B: Internalized phage DNA in lysates of TLR4/CD14/MD2 overexpressing HEK cells incubated with wild type untargeted (WT), EGF-targeted (EGF-phage) or ECRG4$^{(133–148)}$ –targeted (CΔ16-phage) were quantified by Real-Time PCR (qPCR).

Panel C: Internalized phage DNA in lysates of TNFα/IL-1β receptor overexpressing HEK cells incubated with wild type untargeted (WT), EGF-targeted (EGF-phage) or ECRG4$^{(133–148)}$ –targeted (CΔ16-phage) were quantified by Real-Time PCR (qPCR).

Panel D: ECRG4(133–146) was added to the HEK-blue TLR4 reporter cell line at the indicated concentrations either alone (open squares) or at a concentration of 100ng/ml at the

same time as different concentrations of LPS (closed squares). The results were compared to the effects of LPS alone (closed circles)

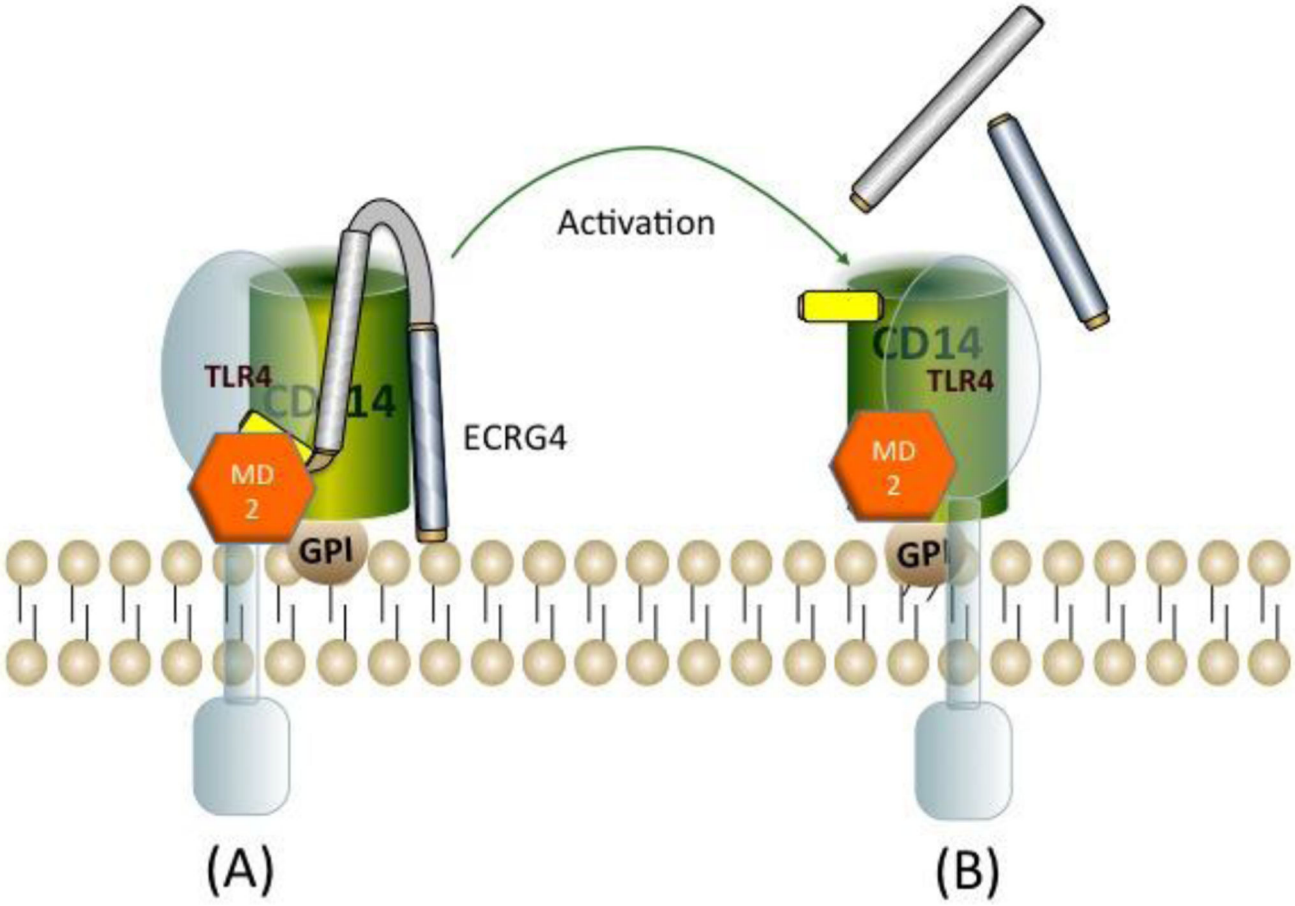

Figure 5. A schematic model of the interaction, binding and internalization of ECRG4 to the TLR4/CD14/MD2 innate immunity receptor complex

Panel A: In the quiescent cells, a membrane tethered ECRG4 precursor physically interacts the TLR4/CD14/MD2 complex presumably by interaction with the C-terminus ECRG4$^{(133–148)}$ moiety. The signal is most likely inhibitory and aimed to gauge responsiveness.

Panel B: With cell activation, ECRG4 processed at the cell surface releases peptides one of which, ECRG4$^{(133–148)}$ interacts with components of the TLR4/CD14/MD2 complex and can internalize into cells.